

Synthesis of N-Acetylglucosamine Derivatives as Anti-Adhesion Molecules for Bacterial Biofilms

Emma Founds
Department of Chemistry and Biochemistry
The University of North Carolina Asheville
One University Heights
Asheville, North Carolina 28804 USA

Faculty Advisor: Dr. Caitlin McMahon

Abstract

Antibiotic resistance has become a global health threat, and with more bacteria becoming resistant to antibiotic drugs, novel strategies to fight infection are needed. Antivirulence as a strategy differs from others as it focuses on blocking virulence factors instead of directly killing the bacteria. One prominent virulence factor is biofilm formation, which initially occurs when bacteria adhere to the surface of a host cell through lectin-carbohydrate binding. Anti-adhesion strategies aim to stop this binding with synthetic sugars that have higher selectivity for the lectins than the natural ligands. In this research, derivatives of N-acetylglucosamine (GlcNAc) are synthesized as inhibitors to block the F17G and GafD lectins on *Escherichia coli* (*E. coli*) bacteria, therefore preventing the adhesion step of biofilm formation. The amide at C2 of GlcNAc is the target of derivation, and this amide group has been manipulated by changing factors like the length of the carbon chain, sterics, and electronics. To synthesize these derivatives, the amine of glucosamine hydrochloride was protected as an imine, and the hydroxyl groups were acetylated. The amine was selectively deprotected to provide a free amine for derivation. From this amine, hexanoyl, butyryl, and benzoyl amides have been synthesized. Deacetylation of the amide derivatives by first making an O-methyl glycoside has been optimized to restore the hydroxyl groups on the sugar. Once a small library of GlcNAc amide derivatives has been completed, the potential inhibitors will be tested for binding to GafD in an ELISA-like assay, which will contribute to further knowledge of the effectiveness of anti-adhesion strategies against *E. coli* infection.

1. Introduction and Background

Antibiotic resistance is a rapidly increasing problem in the world today. It has become a global health threat as, according to the Center for Disease Control (CDC), 2.8 million people in the U.S. alone are infected by drug resistant bacteria each year, resulting in approximately 35,000 yearly deaths.¹ Many different factors contributed to this growing crisis. The first, and most common, is the overuse of antibiotics. The CDC states that one-third to one-half of antibiotic use in humans is unnecessary. For example, antibiotics are sometimes taken for viral infections instead of bacterial infections, which is not appropriate or effective.² Second, bacteria exist in such large numbers that mutations frequently occur, and as nonresistant cells are killed off, resistant mutants remain and replicate. A third cause of resistance is horizontal gene transfer, in which bacteria pass on genetic information to other cells, conferring antibiotic resistance and allowing resistance to be spread more quickly.³ The development of new antibiotics has also severely slowed, as drug manufacturers do not want to risk a financial loss if these new resistant strains will make their product ineffective. Margaret Chan, Director General of the World Health Organization adds to this by saying, "in terms of new replacement antibiotics, the pipeline is virtually dry, especially for Gram-negative bacteria."⁴ Therefore, new strategies are needed to treat and prevent bacterial infections and overcome antibiotic resistance. Without improvements, infections that were previously easier to treat will require more lengthy and costly treatment, extended hospital stays, and will ultimately be more deadly.

One strategy of increasing importance right now is using antivirulence methods to block virulence factors instead of killing the bacteria.⁴ Virulence factors are a broad term used to refer to any bacterial products that damage the host and promote disease. Some virulence factors include quorum sensing, toxin excretion, and biofilm formation. Antivirulence as a strategy is attractive not only because it disarms the way bacteria cause infection but also because it does not contribute to the selective pressures that lead to antibiotic resistance. Another unwanted side effect of antibiotic drugs is their tendency to kill the beneficial bacteria in the body that is helpful for human health, immune system development, and increased metabolic capabilities. Since the antivirulence strategy does not aim to kill bacteria, it is able to bypass this problem.³ There has already been great success with this strategy. In research done by Ghosh et al. in *The Journal of Infectious Diseases*, they studied macrophage migration inhibitory factor (MIF) produced by protozoan parasites as a virulence factor which exacerbates inflammatory diseases. Specifically, the parasite *Entamoeba histolytica* (*E. histolytica*) was observed due to its correlation with inflammatory diarrhea. To target and block *E. histolytica* MIF, a mouse study was completed using neutralizing antibodies in an add-on strategy with antibiotics. Results showed blockage of this virulence factor yielded a significant decrease in intestinal inflammation and tissue damage.⁵ Botulism, a rare illness causing respiratory issues and paralysis, occurs when the agent *Clostridium botulinum* secretes the botulinum neurotoxin (BoNT). These BoNTs act as virulence factors that promote the disease by attacking the body and disrupting the cholinergic neurons at neuromuscular junctions. The FDA-approved antivirulence treatments for botulism involve immunoglobulins purified from donor plasma to target and neutralize BoNTs. Arnon et al. conducted a decade-long study for the *New England Journal of Medicine* with infants using botulism immune globulin intravenous (BabyBIG). BabyBIG was given to people with suspected botulism after initial BoNT intoxication. Results not only showed a significant decrease in the duration of hospital stay but also a successful prevention of further intoxication.⁶ These preceding studies suggest the antivirulence strategy possesses major potential in the treatment of diseases.

The formation of biofilm is a particular virulence factor leading to increased antibiotic resistance. Among human microbial infections, 60% to 80% are caused by cells growing in biofilm. Biofilms are composed of an extracellular matrix of polysaccharides that act to secure and strengthen organisms against modern drug defense. Essentially, biofilms are a protective layer that form around the cell and increase virulence by utilizing resistance mechanisms. They are one of the main reasons for the increasing difficulty in treating against bacterial infection.⁷ A crucial feature of biofilm formation is adhesion, which is simply bacterial attachment to the surface of a host cell (Figure 1). Next in aggregation, microorganisms will come together and stick to each other. Aggregation can then continue, resulting in the formation of biofilm.⁸ By preventing or inhibiting adhesion, biofilms could be prevented or disrupted, making bacteria easier to treat.

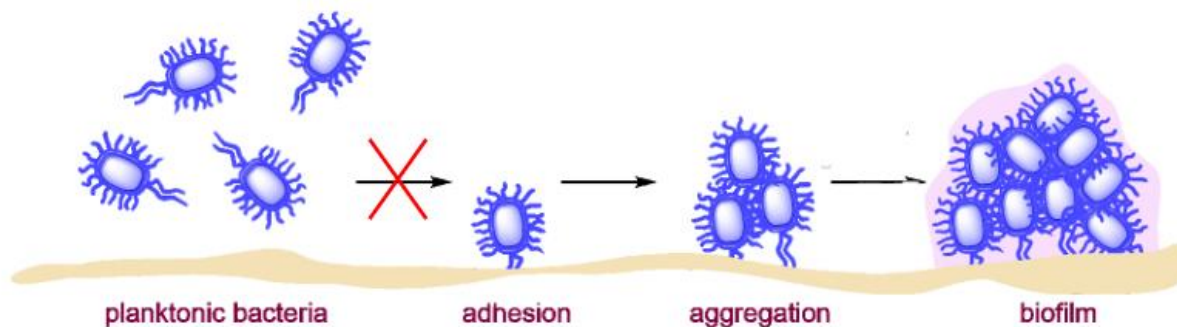


Figure 1. Biofilm formation process, Preventing adhesion halts biofilm formation (McMahon)

Bacterial adhesion occurs due to interactions of tiny hair-like extensions on bacteria called the pili and fimbriae with host cells. At the tips of these pili and fimbriae are lectins, which are carbohydrate-binding proteins. These lectins bind to host carbohydrate ligands with high specificity.⁴ The anti-adhesion process as an antivirulence strategy uses carbohydrate ligands to inhibit the adhesion process, and therefore prevent the formation of biofilm. Naturally occurring sugars have low-affinity for binding to their carbohydrate ligands, but synthesis of rationally designed sugar derivatives could result in ligands with higher binding affinity than the natural sugars.⁹ These synthetic sugars could be used as inhibitors to block the binding site so that the natural sugars cannot bind to it.

Synthesizing high-affinity inhibitors as an antivirulence strategy is not a new technique. Cusumano et al. studied urinary tract infections (UTIs) caused by of Uropathogenic *Escherichia coli* (UPEC). Infections occur in the urinary

tract via adhesion of the FimH lectin at the tips of type 1 pili on UPEC to mannosylated receptors. The goal of the research was to develop high-affinity mannose inhibitors to block bacterial adhesion of the FimH lectin and further prevent infection. Six mannose derivatives were first tested using biofilm inhibition assays and showed promising IC₅₀ values against adhesion. The x-ray crystal structures of FimH bound to mannose was used as rationale for designing their mannosides, and they sought to optimize biphenyl mannosides for this reason (Figure 2). In one case to measure dispersal of biofilm, UTI89 biofilm was grown for 24 hours, then incubated in the presence of mannose derivative six for an additional 16 hours. Confocal microscopy was used and showed a visual decrease in UIT89 biofilm. This showed that these compounds not only affect initial cell adhesion but also disrupt previously existing biofilms. Additional mouse studies were used to determine the *in vivo* capabilities of the mannose inhibitors. The mice were dosed with a mannose derivative 30 minutes before being infected with UTI89. Six hours after infection, the bladders were processed, and confocal microscopy was again used to conclude UPEC infection was absent or rarely seen. These findings lay the groundwork for future development of carbohydrate-based anti-adhesive drugs with specific focus on preventing *E. coli* UTIs.¹⁰

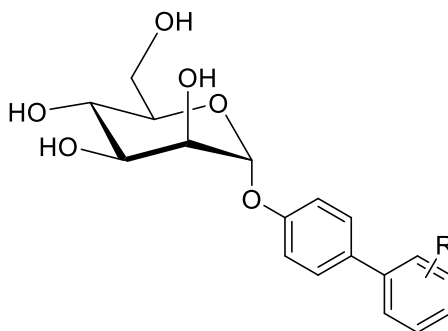


Figure 2. Biphenyl mannose derivative

Though this research has been successful in the past, lesser-known lectins F17G and GafD have yet to be explored as anti-virulence targets. These lectins exist on the strains of *E. coli* associated with diarrheal illness, and they bind to the natural glucose derivative N-acetyl-β-D-glucosamine.^{11,12} These lectins are almost identical, but they are referred to as two different names based on the host organism studied. F17G was identified in infected livestock, while GafD was identified in human hosts. Visually, the F17G lectin shows the immunoglobulin-like fold of the structural components of the fimbriae. The lectin domain has an elongated shape due to its two sheets, a back sheet with five long strands and a front sheet with four antiparallel strands. In the binding site, the interaction between F17G and N-acetyl-β-D-glucosamine occurs through up to eleven hydrogen bond interactions as well as hydrophobic stacking.¹¹ GafD is suggested to have a dual role as a lectin and an assembly protein. The N-terminus participates in receptor recognition, and the C-terminus participates in biogenesis and integration.¹² Bacterial adhesion occurs when these lectins bind to N-acetylglucosamine on the surface of an epithelial cell. Effective inhibitors have not yet been developed for the F17G and GafD lectins.

The goal of this research is to synthesize derivatives of N-acetylglucosamine (GlcNAc) as high-affinity inhibitors of the F17G/GafD lectins, blocking adhesion of the bacteria to host cells (Figure 3). Specifically, the amide group on C2 of the GlcNAc structure will be modified (Figure 4). When observing the F17G protein, the amide position of GlcNAc has the possibility of extending out and around the protein (Figure 5).¹¹ Extending the surface of the sugar could maximize interactions with the protein, which would create stronger binding overall. Thus, the rationale for modifications and designing these sugars are extending the amide through manipulation of factors like sterics and electronics. One example is a carbon chain, which would increase the hydrophobic interactions with the protein's nonpolar residues. Adding an aromatic group might increase the pi-stacking interactions with aromatic amino acids, while also giving a good base to add an oxygen or nitrogen group that may increase hydrogen bonding. Once a small library of GlcNAc amide derivatives is synthesized, all inhibitors will be tested for binding affinity in an enzyme-linked immunosorbent assay (ELISA).

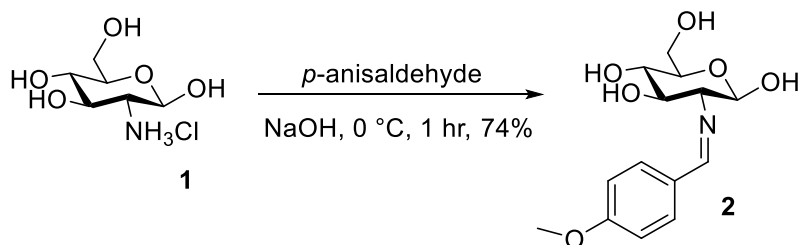
2. Experimental Methods

2.1 General Methods

All chemical reagents were purchased from commercially available sources. Anhydrous solvents were dried over molecular sieves and collected from a solvent system. Reaction progress was monitored using thin layer chromatography (TLC) on SiliaPlates, and UV light or potassium permanganate stain (KMnO_4) was used to visualize. Reactions were concentrated using a Heidolph rotary evaporator. Purification was done via precipitation, filtration, and column chromatography using columns of silica (SiO_2 40-63 μm , 230-400 mesh). Product characterization was done using proton nuclear magnetic resonance (^1H NMR 400 MHz Varian spectrometer) spectroscopy with standards CDCl_3 at 7.27 ppm and d_6 -DMSO at 2.50 ppm. ^1H NMR data reported as follows: chemical shift, multiplicity (s = singlet, d = doublet, t = triplet, q = quartet, quin = quintet, sxt = sextet, dd = doublet of doublets, ddd = doublet of doublets of doublets, dt = doublet of triplets, td = triplet of doublets, qd = quartet of doublets, m = multiplet, br. s. = broad singlet), coupling constants (Hz), integration, and proton identifier.

2.2 Synthesis of (2S, 3R, 4R, 5S, 6R)-6-(acetoxymethyl)-3-aminotetrahydro-2H-pyran-2, 4, 5-triyl triacetate **5**¹³

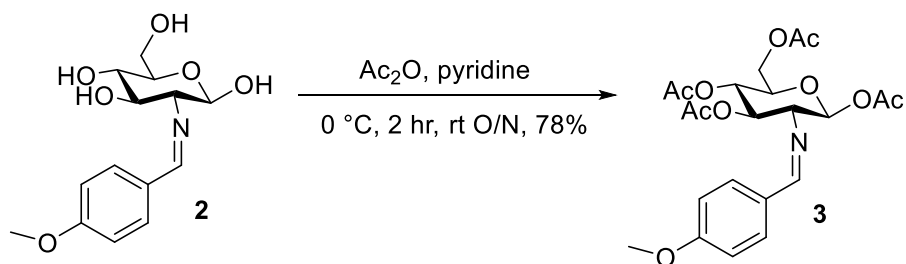
2.2.1 N-Protection of glucosamine hydrochloride as imine **2**



Scheme 1. Synthesis of product **2**

Glucosamine hydrochloride **1** (1.0 equiv, 23.19 mmol, 5.0016 g) was added to 1M aqueous sodium hydroxide (25 mL) under an inert atmosphere using an argon balloon. *p*-Anisaldehyde (25.51 mmol, 3.10 mL) was added dropwise to the solution and left to stir for one hour at 0 °C. The product was filtered using vacuum filtration then rinsed with ice cold water, ethanol, and diethyl ether. Vacuum filtration was completed a second time, rinsing with ice-cold ethanol and ether. The product was left to dry on high vacuum for several hours, resulting in 5.1144 g of **2** as a white solid (74% yield). ^1H NMR (400 MHz, d_6 -DMSO) δ = 8.1 (1H, s), 7.7 (2H, m), 7.0 (2H, m), 3.8 (3H, s), 3.3 (1H, m). The spectra matched the literature values according to Biswas et al.¹³

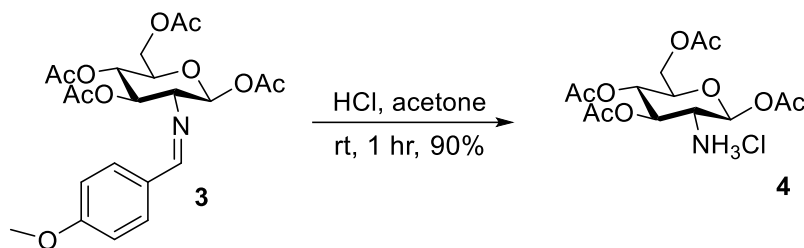
2.2.2 Acetylation of hydroxyl groups to form protected glucosamine derivative **3**



Scheme 2. Synthesis of product **3**

Pyridine (20 mL) was added via syringe to imine **2** (1.0 equiv, 13.45 mmol, 4.0001g). The reaction was left to stir in inert atmosphere using an argon balloon at 0 °C. After 5 minutes, acetic anhydride (4.1 equiv, 55.19 mmol, 5.20 mL) was added. The reaction was left to stir for one hour, more ice was added, and the reaction was left to stir warming to room temperature gradually overnight. The reaction was quenched by adding DI water (50 mL) to the solution at 0 °C. The solution was cooled in an ice bath and more water was added. The contents were vacuum filtered, rinsed with cold water, and left on high vacuum, resulting in 4.8982 g of **3** as a white solid (78% yield). ¹H NMR (400 MHz, *d6*-DMSO) δ = 8.3 (1H, s), 7.7 (2H, d), 7.0 (2H, d), 6.1 (1H, d), 5.4 (1H, t), 5.0 (1H, t), 4.2 (2H, m), 4.0 (1H, m), 3.8 (3H, s, OMe), 3.4 (1H, dd), 2.0 (3H, s), 1.9 (6H, s), 1.8 (3H, s). The spectra matched the literature values according to Biswas et al.¹³

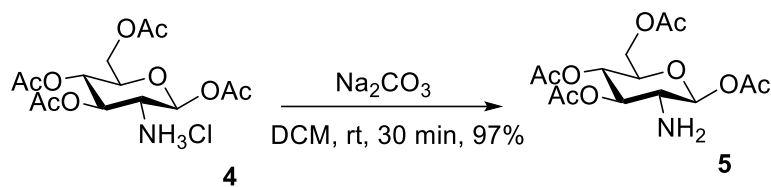
2.2.3 Deprotection of acetoxy imine **3** to form amine **4**



Scheme 3. Synthesis of product **4**

Acetone (33 mL) was added to acetoxy imine **3** (1.0 equiv, 8.59 mmol, 4.0083 g). The reaction was stirred at room temperature and 5 M hydrochloric acid (2 mL) was added. After 30 minutes, diethyl ether was added, and solution was left to stir for 1 hour. The product was vacuum filtered, rinsed with cold diethyl ether, and dried on the high vacuum, resulting in 2.9597 g of **4** as a white solid (90% yield). ¹H NMR (400 MHz, *d6*-DMSO) δ = 5.9 (1H, d), 5.35 (1H, t), 4.9 (1H, t), 4.2 (1H, dd), 4.1 (1H, m), 4.0 (1H, m), 3.6 (1H, t), 2.15 (4H, s), 2.0 (13H, m). The spectra matched the literature values according to Biswas et al.¹³

2.2.4 Deprotection of amine **4** to form neutral amine **5**

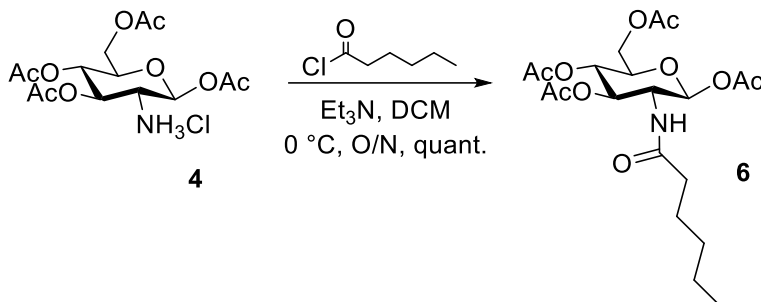


Scheme 4. Synthesis of product **5**

Dichloromethane (17 mL) was added to acetoxy glucosamine hydrochloride **4** (1.0 equiv, 2.61 mmol, 1.0075 g). Aqueous sodium carbonate (10% w/v, 10 mL) was slowly pipetted into the reaction and left to stir for 30 minutes. The organic layer was then separated from the top aqueous layer. The aqueous layer was extracted with dichloromethane. The combined organic layers were dried using magnesium sulfate and filtered. The reaction was concentrated by rotary evaporation and dried under high vacuum, resulting in 0.8783 g of **5** as a white solid (97% yield). ¹H NMR (400 MHz, *d6*-DMSO) δ = 5.5 (1H, t), 5.0 (1H, t), 4.8 (1H, t), 4.15 (1H, dd), 3.95 (2H, m), 2.7 (1H, dd), 2.1 (3H, m), 1.95 (9H, m). The spectra matched the literature values according to Biswas et al.¹³

2.3 Synthesis of Amide Derivatives **6**, **7**, **8**¹⁴

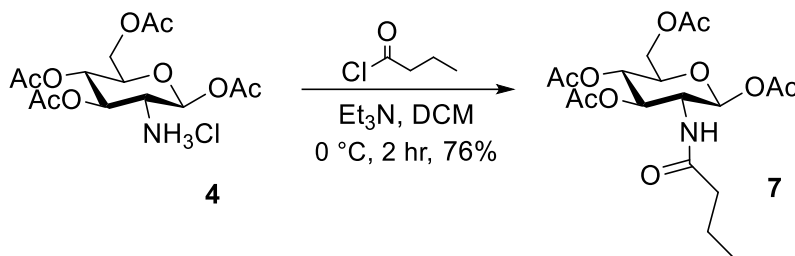
2.3.1 Addition of hexanoyl chloride



Scheme 5. Acyl chloride reaction using hexanoyl chloride

A solution of acetoxycyclohexylamine hydrochloride **4** (1.0 equiv, 2.61 mmol, 1.0062 g) and dry dichloromethane (1 equiv, 2.61 mmol, ~15 mL) started stirring under an inert atmosphere using an argon balloon. Triethylamine (2 equiv, 5.22 mmol, 0.7 mL) was added, and the reaction was cooled to 0 °C. Hexanoyl chloride (1.2 equiv, 3.34 mmol, 0.45 mL) was added dropwise, and the reaction was left to stir overnight. Ethyl acetate (70 mL) was added to the reaction. The organic layer was washed with DI water, 1M sodium hydroxide, and saturated sodium chloride (brine). The organic layer was dried using magnesium sulfate and filtered. The reaction was concentrated by rotary evaporation, resulting in 1.1812 g of **6** as a white solid (quant). ¹H NMR (400 MHz, CDCl₃) δ = 5.7 (1H, d), 5.4 (1H, d), 5.2 (2H, m), 4.3 (2H, m), 4.1 (2H, m), 3.8 (1H, m), 2.1 (14H, m), 1.6 (2H, m), 1.3 (6H, m), 0.9 (3H, t). The spectra matched the literature values according to Macauley et al.¹⁴

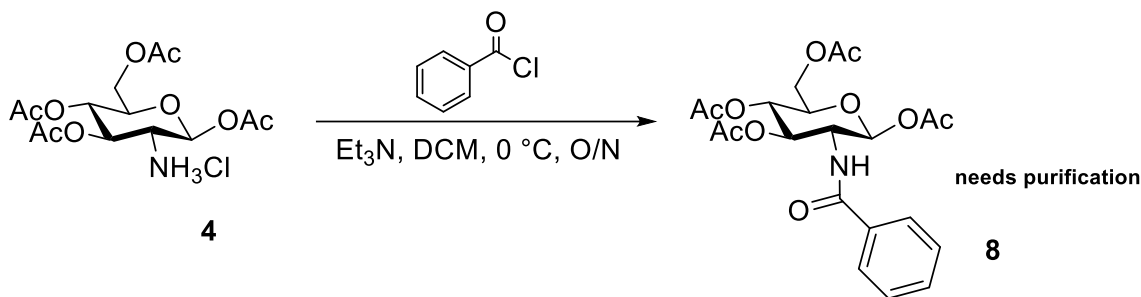
2.3.2 Addition of butyryl chloride



Scheme 6. Acyl chloride reaction using butyryl chloride

A solution of acetoxycyclohexylamine hydrochloride **4** (1.0 equiv, 0.782 mmol, 0.300 g) and dry dichloromethane (0.782 mmol, ~4 mL) was stirred under an inert atmosphere using an argon balloon. Triethylamine (2 equiv, 1.56 mmol, 0.2 mL) was added, and the reaction was cooled to 0 °C. Butyryl chloride (1.2 equiv, 0.939 mmol, 0.1 mL) was added dropwise, and the reaction was left to stir for 2 hours. Ethyl acetate (~25 mL) was added to the reaction. The organic layer was washed with DI water, 1M sodium hydroxide, and saturated sodium chloride (brine). The organic layer was dried using magnesium sulfate and filtered. The product was purified via column chromatography in 5:1 ethyl acetate and hexane, and concentrated by rotary evaporation, resulting in 0.2465 g of **7** as a white solid (76%). ¹H NMR (400 MHz, CDCl₃) δ = 5.7 (1H, d, NH), 5.4 (1H, m), 5.1 (2H, m), 4.4 (1H, ddd), 4.3 (1H, dd), 4.1 (1H, d), 3.8 (1H, ddd), 2.1 (14H, m), 1.6 (8H, ddd), 1.0 (3H, t). The spectra matched the literature values according to Macauley et al.¹⁴

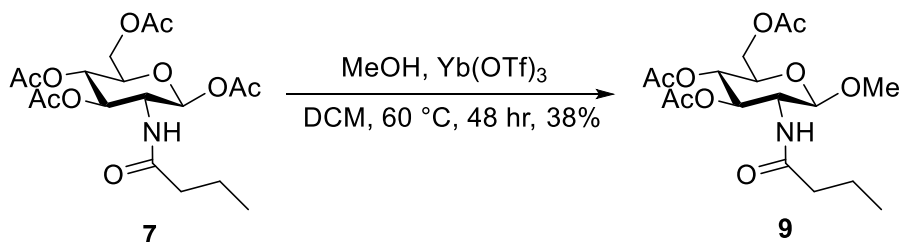
2.3.3 Addition of benzoyl chloride



Scheme 7. Acyl chloride reaction using benzoyl chloride

A solution of acetoxy glucosamine hydrochloride **4** (1.0 equiv, 0.782 mmol, 0.300 g) and dry dichloromethane (1 equiv, 0.782 mmol, ~4 mL) was stirred under an inert atmosphere using an argon balloon. Triethylamine (2 equiv, 1.56 mmol, 0.22 mL) was added, and the reaction was cooled to 0 °C. Benzoyl chloride (1.2 equiv, 0.94 mmol, 0.1 mL) was added dropwise, and the reaction was left to stir overnight. Ethyl acetate (~25 mL) was added to the reaction. The organic layer was washed with DI water, 1M sodium hydroxide, and saturated sodium chloride (brine). The organic layer was dried using magnesium sulfate and filtered. The product was purified via column chromatography in 1:1 ethyl acetate and hexane and concentrated by rotary evaporation. The ¹H NMR showed excess benzoyl chloride, so further purification using either another column or a prep LC is needed.

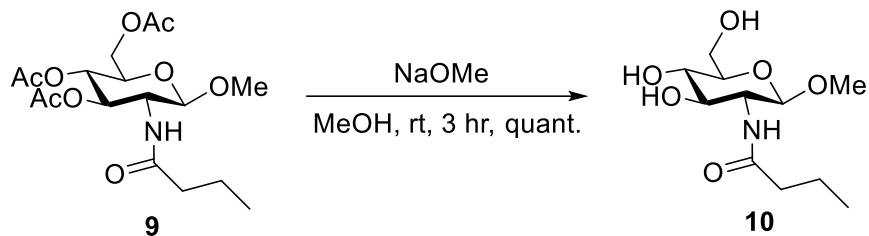
2.4 Synthesis of O-methyl glycoside **9** of per-acetylated butyl derivative **9**¹⁵



Scheme 8. O-Methylation reaction to anomeric carbon

Dry dichloromethane (2.5 mL) was added to per-acetylated butyl derivative **7** (1.0 equiv, 0.2396 mmol, 0.1010 g). Ytterbium (III) triflate hydrate (0.12 equiv, 0.0288 mmol, 0.0224 g) and dry methanol (0.15 mL) were added, and reaction was left to reflux overnight at 60 °C under an inert atmosphere. Additional dry methanol (0.15 mL) was added, and reaction was left to stir for another 24 hours. Reaction was then cooled to room temperature, and the organic layer was washed three times with deionized water. The organic layer was dried using magnesium sulfate and filtered. The product was purified via column chromatography in 3:2 ethyl acetate and hexane and concentrated by rotary evaporation to yield 0.0359 g of **9** as a white solid (38%). ¹H NMR (400 MHz, CDCl₃) δ = 5.5 (1H, d), 5.3 (2H, m), 5.1 (2H, m), 4.6 (1H, d), 4.3 (2H, m), 4.1 (1H, m), 3.9 (1H, m), 3.7 (1H, m), 3.5 (3H, s), 2.1 (7H, m), 2.0 (8H, m), 1.3 (1H, s), 0.9 (5H, m).

2.5 Deacetylation of methylated butyl derivative¹⁵

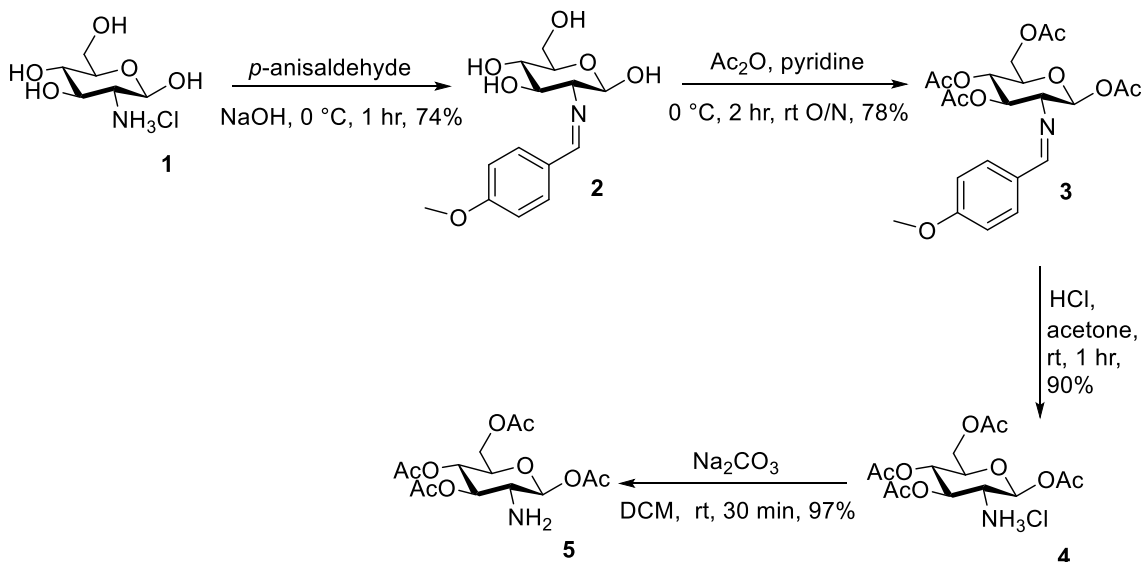


Scheme 9. Deprotection of acetyl functional groups

A solution of protected methylated butyl product **9** (1.0 equiv, 0.0770 mmol, 0.0248 g) and dry methanol (1 mL) started stirring in an inert atmosphere using an argon balloon. Sodium methoxide solution (3.0 equiv, 0.5 M, 0.5 mL) was added, and the reaction was left to stir under argon at room temperature for 3 hours. Two small scoops of Amberlite IR-120 (H) resin (pre-washed with 1M HCl and DI water) were added to the reaction and left to stir for 30 minutes. This was repeatedly done until the pH of the reaction was neutral. The resin was filtered out, and the reaction was concentrated by rotary evaporation to yield 0.0330 g of **10** a white clear solid (quant). ¹H NMR (400 MHz, *d*₆-DMSO) δ = 7.6 (1H, d, NH), 4.9 (1H, s), 4.6 (1H, t), 4.2 (1H, d), 2.0 (3H, m), 1.5 (3H, m), 0.8 (5H, m).

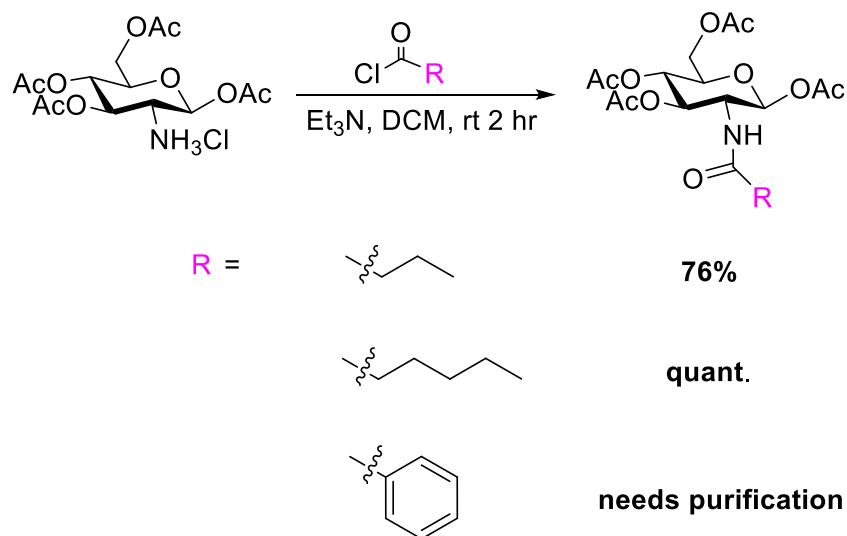
3. Results and Discussion

Before derivatizing the amide, the nitrogen needed to be protected so that differential protection of the hydroxy groups of C1, C3, C4, and C6 could occur. This was done through imine protection and O-acetylation according to Biswas et al. (Scheme 10).¹³ Removal of the imine was then completed to selectively deprotect the nitrogen to prepare it for reactivity. From this O-protected amine intermediate, GlcNAc amide derivatives were synthesized via coupling reactions with acyl chlorides. In this manner, a hexyl derivative, butyl derivative, and benzoyl derivative have been made to manipulate the sterics and electronic properties of the amide group. Future derivations will be made to investigate further manipulation of electronics.



Scheme 10. Selective acetylation of glucosamine hydrochloride

Overall, there was great success in the protection scheme of synthesizing O-protected glucosamine **4** and **5**. ¹H NMR data matched previously reported spectra, and the products were obtained in high yields and purity in the form of white solids. The addition of a hexyl and butyl chains onto the amide position by reaction with the acyl chlorides also resulted in good yields of amide derivatives. The addition of the benzoyl group was also successful but proved more difficult to purify (Scheme 11). High performance liquid chromatography (HPLC) is being investigated as an alternative purification method for this UV-active compound.



Scheme 11. Synthesis of butyl, hexyl, and benzoyl amide derivatives

From here, we began troubleshooting the deprotection of the acetyl groups and purification of final inhibitor compounds. Deprotecting carbons 1, 3, 4, and 6 all at once resulted in reaction mixtures that were difficult to purify and characterize. By deprotecting anomeric glycosides of GlcNAc previously synthesized in the McMahon group, it was found that deprotections are much easier to carry out when the anomeric carbon is locked in the β position as an acetal, rather than a hemi-acetal. Because of this, O-methyl glycosides of the amide derivatives were synthesized to facilitate easier deprotection and purification. Not only will this lock this carbon in the β position but this will also decrease the number of acetyl groups to be deprotected from four to three and result in a slightly less polar compound, hopefully leading to easier purification. While making the O-methyl glycoside, we had trouble keeping the methanol in the heated flask, so we first lowered the reflux temperature to 50 °C. However, this then led to an excess of unreacted starting material. To prevent this, the temperature was then increased back to 60 °C, and the reaction time was increased from 24 to 48 hours. More methanol was also added to ensure that enough would stay in the flask and be able to react with the starting material. This successfully produced the O-methyl glycoside, which was then successfully used as the starting material for the deprotection reaction, which also produced more promising results.

In combination with synthesis, the lectin proteins were expressed and purified by another member of the McMahon lab. To do this, a DNA plasmid was constructed using restriction enzymes and ligation to insert the gene encoding for GafD into a vector. Then, the plasmid was sequenced to confirm gene insertion, the plasmid was transformed into *E. coli*, and then the bacteria were cultured to express the protein. Affinity chromatography was used for purification, and proteins were assessed using SDS-PAGE gel electrophoresis and binding assays.

Future directions for this research include synthesis of additional GlcNAc derivatives. The butyl, hexyl, and benzyl derivatives not only provide an excellent start for increasing hydrophobic and pi-stacking interactions with the protein, but the established synthetic routes also provide a means to obtain additional amide derivatives. For example, longer carbon chains can be added to the sugar via the acyl chloride reaction, and oxygen or nitrogen groups can be added to the benzyl derivative to test whether additional hydrogen bonding interactions would be possible. After a small library of GlcNAc derivatives is completed, an enzyme-linked immunosorbent assay (ELISA) will be used to test the binding affinity of our inhibitors versus the natural GlcNAc ligand (Figure 6). The final step of the ELISA assay is a wash step, followed by addition of antibodies that are linked to an enzyme to cause a color change if they detect the protein. This color change would indicate that our inhibitors are low-affinity, as the F17G lectin bound to the naturally occurring GlcNAc. High-affinity inhibitors would result in no color change, as the lectin bound to the inhibitor and was washed away.

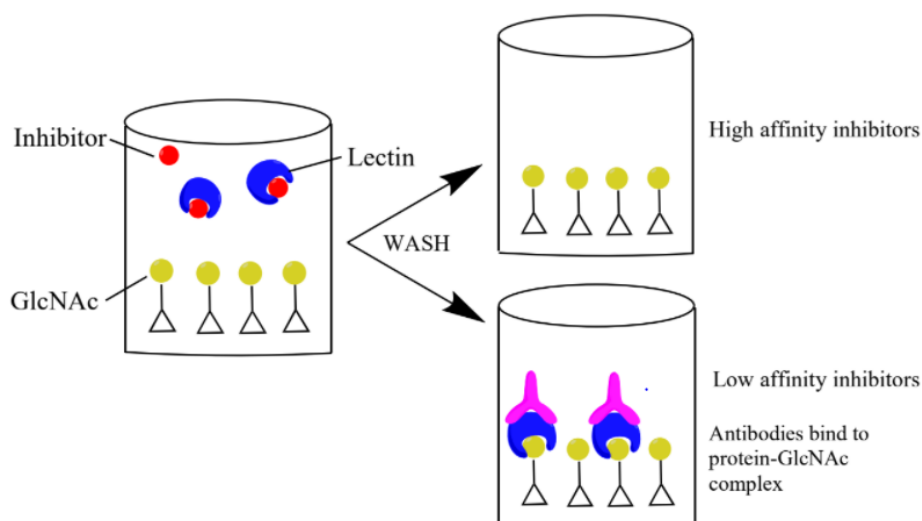


Figure 6. ELISA assay for determining affinity of synthetic inhibitors against the natural GlcNAc ligand (Pistor)

4. Conclusion

Three amide derivatives of GlcNAc have been synthesized: butyl, hexyl, and benzyl derivatives. Starting material for these derivatives was made by protecting the amine of glucosamine hydrochloride with an imine, acetylating the hydroxyl groups, and then selectively deprotecting the amine, making the amine free for derivation. An acyl chloride reaction using butyryl, hexanoyl, and benzoyl chlorides was completed to make the three current amide derivatives. Deprotection of these derivatives has been optimized by synthesizing the O-methyl glycoside using ytterbium (III) triflate hydrate as a catalyst, then proceeding with the deacetylation using sodium methoxide solution and methanol. An ELISA assay will be used to evaluate the binding affinity of the inhibitors to F17G/GafD lectins and compare them to the binding affinity of the naturally occurring GlcNAc ligand through competition experiments. These results will indicate how effective the synthetic inhibitors are at attaching to the lectins and preventing the naturally occurring GlcNAc from adhering to them. If the natural GlcNAc cannot adhere to the F17G/GafD lectin, then adhesion will not be able to occur, so the formation of biofilm cannot be carried out. With the absence of biofilm around the bacteria, the bacteria's antibiotic resistance will significantly decrease, and it will be easier to eradicate. This antivirulence strategy sets a foundation for future research on *E. coli* adhesins and their ability to combat antibiotic resistance through inhibition of bacterial biofilm.

5. Acknowledgements

I would like to thank Dr. McMahon for all her support, the McMahon research lab for the space and materials to carry out this research, and the UNCA Department of Chemistry and Biochemistry.

6. References

1. Services, U. D. of H. and H. Antibiotic Resistance Threats in the United States. *Centers Dis. Control Prev.* **2019**, 1-113.
2. Antibiotics: Are You Misusing them? *Mayo Clinic.* **2020**.
3. Dickey, S. W.; Cheung, G. Y. C.; Otto, M. Different Drugs for Bad Bugs: Antivirulence Strategies in the Age of Antibiotic Resistance. *Nature Reviews Drug Discovery* **2017**, 16 (7), 457-471.

4. Sommer, R.; Joachim, I.; Wagner, S.; Titz, A. New Approaches to Control Infections: Anti-Biofilm Strategies against Gram-Negative Bacteria. *CHIMIA International Journal for Chemistry* **2013**, *67* (4), 286–290.
5. Ghosh, S.; Padalia, J.; Ngobeni, R.; Abendroth, J.; Farr, L.; Shirley, D. A.; Edwards, T.; Moonah, S. Targeting Parasite-Produced Macrophage Migration Inhibitory Factor as an Antivirulence Strategy with Antibiotic-Antibody Combination to Reduce Tissue Damage. *J. Infect. Dis.* **2020**, *221* (7), 1185-1193.
6. Arnon, S. S., Schechter, R., Maslanka, S. E., Jewell, N. P. and Hatheway, C. L. Human botulism immune globulin for the treatment of infant botulism. *N. Engl. J. Med.* **2006**, *354*, 462-471.
7. Korea, C., Ghigo, J. and Beloin, C. The sweet connection: Solving the riddle of multiple sugar-binding fimbrial adhesins in Escherichia coli. *Bioessays*, **2011**, *33*: 300-311.
8. Crouzet, Marc; Le Senechal, Caroline; Brözel, Volker S; Costaglioli, Patricia; Barthe, Christophe; Bonneu, Marc; Garbay, Bertrand; Vilain, Sebastien. Exploring early steps in biofilm formation: set-up of an experimental system for molecular studies. *BMC Microbiology*, **2014**, *14*(1), 253.
9. Sharon, N. Carbohydrates as Future Anti-Adhesion Drugs for Infectious Diseases. *Biochimica et Biophysica Acta (BBA) – General Subjects* **2005**, *1760* (4), 527-537.
10. Cusumano, C. K.; Pinkner, J. S.; Han, Z.; Greene, S. E.; Ford, B. A.; Crowley, J. R.; Henderson, J. P.; Janetka, J. W.; Hultgren, S. J. Treatment and Prevention of Urinary Tract Infection with Orally Active FimH Inhibitors. *Sci. Transl. Med.* **2011**, *3* (109).
11. Buts, L., Bouckaert, J., De Genst, E., Loris, R., Oscarson, S., Lahmann, M., ... De Greve, H. The fimbrial adhesin F17-G of enterotoxigenic Escherichia coli has an immunoglobulin-like lectin domain that binds N-acetylglucosamine. *Molecular Microbiology*, **2004**, *49*(3), 705–715.
12. Saarela, S., Taira, S., Nurmiäho-Lassila, E. L., Makkonen, A., & Rhen, M. The Escherichia coli G-fimbrial lectin protein participates both in fimbrial biogenesis and in recognition of the receptor N-acetyl-D-glucosamine. *Journal of Bacteriology*, **1995**, *177*(6), 1477–1484.
13. Biswas, N. N.; Yu, T. T.; Kimyon, Ö.; Nizalapur, S.; Gardner, C. R.; Manefield, M.; Griffith, R.; Black, D. S. C.; Kumar, N. Synthesis of Antimicrobial Glucosamides as Bacterial Quorum Sensing Mechanism Inhibitors. *Bioorganic Med. Chem.* **2017**, *25* (3), 1183-1194.
14. Macauley, M. S.; Whitworth, G. E.; Debowski, A. W.; Chin, D.; Vocadlo, D. J. O-GlcNAcase Uses Substrate-Assisted Catalysis: Kinetic Analysis and Development of Highly Selective Mechanism-Inspired Inhibitors. *J. Biol. Chem.* **2005**, *280* (27), 25315-15322.
15. Schultz, V. L.; Zhang, X.; Linkens, K.; Rimel, J.; Green, D. E.; Deangelis, P. L.; Linhardt, R. J. Chemoenzymatic Synthesis of 4-Fluoro-N Acetylhexosamine Uridine Diphosphate Donors: Chain Terminators in Glycosaminoglycan Synthesis. *J. Org. Chem.* **2017**, *82* (4), 2243-2248.